

# Surface-enhanced Raman scattering: a new optical probe in molecular biophysics and biomedicine

Janina Kneipp · Burghardt Wittig ·  
Henrik Bohr · Katrin Kneipp

Received: 13 July 2009 / Accepted: 16 October 2009 / Published online: 13 November 2009  
© Springer-Verlag 2009

**Abstract** Sensitive and detailed molecular structural information plays an increasing role in molecular biophysics and molecular medicine. Therefore, vibrational spectroscopic techniques, such as Raman scattering, which provide high structural information content are of growing interest in biophysical and biomedical research. Raman spectroscopy can be revolutionized when the inelastic scattering process takes place in the very close vicinity of metal nanostructures. Under these conditions, strongly increased Raman signals can be obtained due to resonances between optical fields and the collective oscillations of the free electrons in the metal. This effect of surface-enhanced Raman scattering (SERS) allows us to push vibrational spectroscopy to new limits in detection sensitivity, lateral resolution, and molecular structural selectivity. This opens up exciting perspectives also in molecular biospectroscopy. This article highlights three directions where SERS can

offer interesting new capabilities. This includes SERS as a technique for detecting and tracking a single molecule, a SERS-based nanosensor for probing the chemical composition and the pH value in a live cell, and the effect of so-called surface-enhanced Raman optical activity, which provides information on the chiral organization of molecules on surfaces.

**Keywords** Nanosensor · Raman spectroscopy · Cells · Single molecule · Plasmonics

## 1 Introduction

Most of optical and spectroscopic tools in biophysical and biomedical research, which are currently in use are based on fluorescence spectroscopy. Methods can exploit intrinsic fluorescence of the biological object, but, in most cases, objects of biomedical interest, such as cells, proteins, or others are labeled with organic dye molecules or quantum dots, which act as reporter species providing stronger and more specific fluorescence signals than biomolecules [1, 2]. But also in case of intrinsic fluorescence signals originating from the biomolecules, the information on molecular structure and chemical composition of the biological target object is limited. Therefore, an important challenge in biospectroscopy is to develop optical tools, which also deliver molecular structural information on biological samples, particularly also sensitive information on molecular structural changes. Such information can provide new insight into biophysical and biochemical processes and a deeper understanding of the development of diseases at a molecular level.

In general, detailed molecular structural information can be provided by the vibrational spectrum. The energy

---

Dedicated to Professor Sandor Suhai on the occasion of his 65th birthday and published as part of the Suhai Festschrift Issue.

---

J. Kneipp (✉)  
Federal Institute for Materials Research and Testing,  
Berlin, Germany  
e-mail: janina@janina-kneipp.de

J. Kneipp  
Chemistry Department,  
Humboldt University Berlin, Berlin, Germany

B. Wittig · K. Kneipp  
Institute of Molecular Biology and Bioinformatics,  
Charité University Medicine, Berlin, Germany

H. Bohr · K. Kneipp  
Physics Department, Danish Technical University,  
Lyngby, Denmark  
e-mail: katrin.kneipp@fysik.dtu.dk

of the vibrational levels is determined by the kind of atoms and bonding strengths between them. The symmetry of the molecule determines the transition matrix elements, i.e., signal strength of specific vibrational modes in a spectrum.

Molecular vibrations can be probed by infrared (IR) absorption spectroscopy or by inelastic scattering of photons from vibrational quantum states, called Raman scattering. The frequency shift between incoming and Raman scattered light is determined by the energy of molecular vibrations. Depending on the applied wavelength for excitation, in Raman spectroscopy, information on molecular vibrational frequencies is transferred from the IR energy range to the visible, near ultra violet, or near infrared range, respectively, where some technical advantages, such as sensitive detectors, notch filters, better light sources, fiber-optic probes, combination of Raman spectroscopy, and microscopy etc. exist [3]. These improvements are of interest, particularly also for biomedical applications of Raman spectroscopy [4–8].

In general, Raman scattering signals are exceedingly weak. Typical Raman cross sections range between  $10^{-30}$  and  $10^{-25}$  cm<sup>2</sup>, with the larger values occurring during resonant Raman conditions. In exceptional situations for some dyes, resonant Raman cross sections can reach  $10^{-23}$  cm<sup>2</sup>. In comparison, fluorescence exploits cross sections of about  $10^{-16}$  cm<sup>2</sup>, IR-absorption cross sections are between  $10^{-20}$  and  $10^{-17}$  cm<sup>2</sup>.

However, the situation for Raman scattering totally changes when the inelastic scattering process takes place in the very close vicinity of metal nanostructures. Now strongly increased Raman signals can be obtained, which occur mainly due to resonances between optical fields and the collective oscillations of the free electrons in a metal. This effect of surface-enhanced Raman scattering (SERS) allows to push vibrational spectroscopy to new limits in sensitivity, molecular structural selectivity, and lateral resolution [9]. This is of particular interest for biological and biomedical applications of Raman scattering [10–19].

Here, after a brief introduction of surface-enhanced Raman scattering, we highlight three directions where SERS can offer interesting new capabilities in molecular biospectroscopy. We discuss SERS as a technique for detection and tracking single biomedically relevant molecules. In a second example, we introduce a SERS-based nanosensor for structurally selective chemical probing and pH measurements in small biological structures, such as cellular compartments. Finally we show that SERS gives rise to interesting new results for the effect of so-called Raman optical activity (ROA), which can be obtained for chiral molecules and has the capability to differentiate between left and right-handed species.

## 1.1 Physics background—a brief introduction to Raman scattering and surface-enhanced Raman scattering

Figure 1 shows a schematic of the Raman scattering (RS) in a molecular energy level diagram. Depending on whether photons interact with a molecule in its vibrational ground or first excited vibrational state, the scattering signals appear at the low energy side (Stokes:  $h\nu_S = h\nu_L - h\nu_M$ ) or high energy side (anti-Stokes:  $h\nu_{aS} = h\nu_L + h\nu_M$ ) of the excitation laser. The scattering signal power  $P_{RS}$  of a Raman line depends on excitation intensity  $I_L$  and the Raman cross section  $\sigma^R$ , where  $\sigma^R$  is determined by the change of the polarizability during the molecular vibration. In general, anti-Stokes Raman scattering results in much lower scattering signals compared to Stokes scattering, because only a small fraction of molecules, determined by the Boltzmann population is in an excited vibrational state and can contribute to anti-Stokes Raman scattering.

In hyper Raman scattering (HRS) two-photons are simultaneously scattered, and thus HRS results in Raman signals shifted relative to the doubled energy of the excitation laser ( $h\nu_{HS} = 2h\nu_L - h\nu_M$  and  $h\nu_{HaS} = 2h\nu_L + h\nu_M$ ). HRS follows symmetry selection rules different from regular one-photon RS, and therefore it can provide additional molecular structural information by probing vibrational modes complementary to those that appear in a “normal” RS spectrum. The power of RS signals  $P_{RS}$  is linearly dependent on the excitation intensity, whereas HRS signals depend on the excitation intensity to the power of two. As a non-linear, incoherent Raman process, HRS is an extremely weak effect with scattering cross sections of the order of  $10^{-65}$  cm<sup>4</sup> s, 35 orders of magnitude smaller than cross sections of “normal” (one-photon-excited) Raman scattering and 15 orders of magnitude below typical two-photon absorption cross sections. These

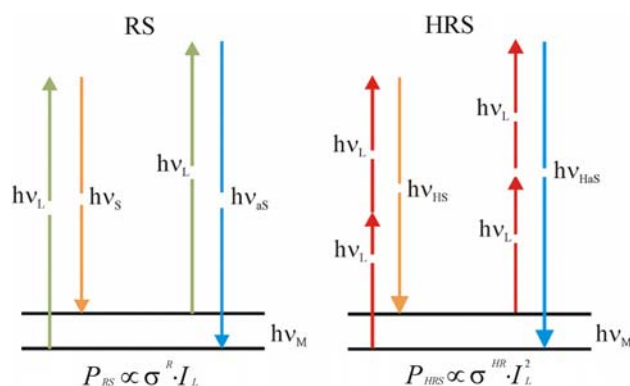


**Fig. 1** Raman (RS) and hyper Raman (HRS) Stokes and anti-Stokes scattering (the right part of each figure displays the Stokes process, the left part the anti-Stokes process)

extremely small cross sections have so far precluded application of HRS as practical spectroscopic tool.

The structural information content of Raman scattering can be further extended to chiral information by exploiting differences in Raman signal strengths obtained for left- and right-circularly polarized light. The effect of ROA measures the normalized difference between scattering signals of right and left circularly polarized excitation and/or scattered light. ROA is introduced as dimensionless circular intensity difference (CID) with  $CID = ({}^R I_R - {}^L I_L) / ({}^R I_R + {}^L I_L)$ . Superscript and subscript R and L indicate right and left circularly polarized excitation and Raman light, respectively. Due to its origin in higher order effects ROA is an extremely weak phenomenon, usually 3–5 orders of magnitude smaller than Raman scattering resulting in CID numbers of  $10^{-3}$  at best [20, 21]. Therefore, extracting ROA spectra from molecules of biological interest requires high excitation powers and long collection times up to hours. Recently, the technique has been pushed to new limits. Instrumental advances in ROA combined with quantum chemical computations made it possible to determine the absolute configuration of chirally deuterated neopentane [22].

Optical effects can be strongly affected when they take place in the immediate vicinity of metal surfaces and nanostructures due to coupling to surface plasmons. Based on resonances with its surface plasmons, gold- and silver nanostructures give rise to enhanced local optical fields, where spectroscopy takes place. This results in enhanced spectroscopic signals. Figure 2 illustrates surface-enhanced Raman scattering schematically. The formula shown in the figure estimates the scattering signal in a SERS experiment. The total Stokes SERS signal  $P_{SERS}$  is proportional to the Raman cross section  $\sigma_{ads}^R$ , the excitation laser intensity  $I_L$

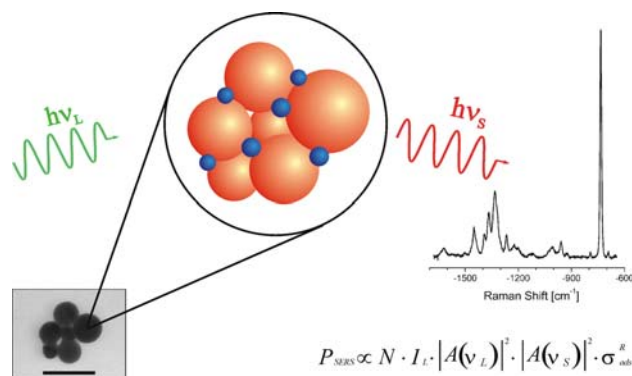


**Fig. 2** Surface-enhanced Raman scattering (schematic) and a SERS spectrum of  $10^{-9}$  M adenine. Molecules (blue dots) are in the close vicinity to gold or silver nanospheres (orange), for comparison see, TEM images of a SERS-active gold nanoaggregate (scale bar is 100 nm). Reprinted with permission from Ref. [9]

and the number of molecules  $N$  involved in the SERS process.

Two effects are operative in this surface-enhanced Raman scattering: The first enhancement mechanism is related to resonances between the surface plasmons of the metal nanostructures and the excitation and scattered fields during the Raman process, giving rise to enhanced local optical fields. So-called field enhancement factors  $A(\nu_L)$  and  $A(\nu_S)$  account for this “electromagnetic” SERS mechanism.

The second enhancement mechanism occurs due to so-called “chemical or electronic effects”, where a molecule in contact with a metal (nanostructure) exhibits a “new Raman process” with a larger cross section than that of a free molecule.  $\sigma_{ads}^R$  describes an enhanced cross section of the adsorbed molecule due to “chemical” SERS enhancement compared to the cross section  $\sigma_{free}^R$  in a “normal” Raman experiment without the presence of metal nanostructures. For more explanation of the origin of “electromagnetic” and “chemical” SERS enhancement see refs. [23–25].

Total enhancement factors obtained in SERS can reach 14 orders of magnitude. In general, the contribution of electromagnetic and chemical enhancement mechanisms to the total SERS effect remains a subject of discussion. However, in many experiments performed on nanometer-scale silver or gold structures, electromagnetic enhancement plays a key role. In the visible and near infrared frequency range, silver and gold nanostructures can result in electromagnetic SERS enhancement factors up to 12 orders of magnitude [26–28].

Electromagnetic enhancement also provides the key effect for the observation of surface-enhanced hyper Raman scattering (SEHRS). Small aggregates, consisting of gold and silver nanoparticles and fractal structures of these metals that provide extremely strong field enhancement, which can give rise to enhancement factors for HRS signals up to 20 orders of magnitude. This results in effective two-photon cross sections similar or higher than the best cross sections for two-photon fluorescence [29]. In general, two-photon spectroscopy provides several advantages over one-photon excitation, including the application of light of a longer wavelength and the limitation of the excitation volume in a sample [30]. These specific characteristics of two-photon excitation are of particular interest for biomedical applications of spectroscopy and microscopy [31–33]. So far, two-photon excitation has been applied in fluorescence spectroscopy. New approaches in two-photon excited surface-enhanced hyper Raman spectroscopy combine the advantages of two-photon spectroscopy with the structural information of vibrational spectroscopy, and the high sensitivity and nanometer-scale local confinement of plasmonics-based spectroscopy [29].

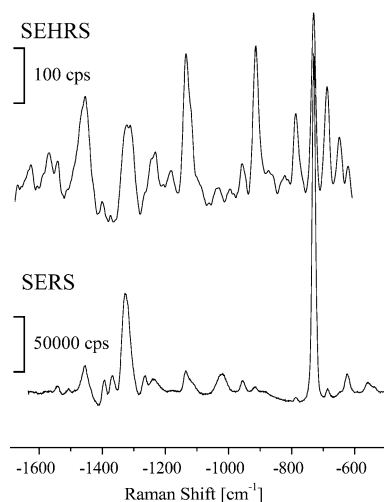


**Fig. 3** SEHRS and SERS spectra of adenine in aqueous solution with silver nanoaggregates. One-photon excited SERS spectra were measured using 514.5 nm cw light, two-photon excited SEHRS spectra were measured using 1,064 nm mode locked ps pulses. Reprinted with permission from Ref. [29]

## 1.2 Ultrasensitive label-free detection and tracking of biomedically relevant molecules

Extremely high SERS enhancement factors allow the ultrasensitive detection and structural identification of molecules based on intrinsic Raman signals. In particular, SERS opens up opportunities for monitoring biologically relevant molecules at the single molecule level [10]. Applications range from Raman spectroscopic characterization of specific DNA fragments down to structurally

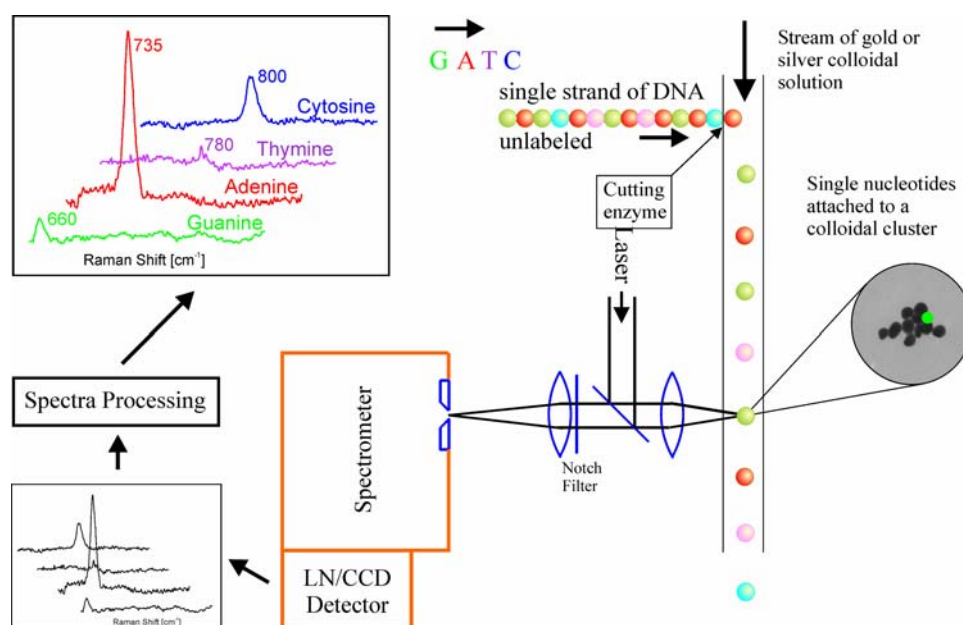
sensitive detection of single DNA bases without the use of fluorescent or radioactive tags, based on the intrinsic surface-enhanced Raman scattering signals [34].

As an example, Fig. 3 displays surface-enhanced Raman spectra of the DNA base adenine using one- and two-photon excitation [29]. Effective SERS cross sections for adenine were shown to be of the order of  $10^{-16} \text{ cm}^2$ . As Fig. 3 shows, strong SEHRS signals are obtained for adenine as well. Compared to the SERS spectrum its SEHRS spectrum shows several additional strong scattering lines that can be ascribed to IR-active vibrations. Effective SEHRS cross sections for adenine have been inferred to be between  $10^{-46}$  and  $10^{-45} \text{ cm}^4 \text{ s}$  ( $=10^4$ – $10^5 \text{ GM}$ ). Figure 3 shows that one-photon SERS cross sections are at the level of fluorescence cross sections of “good” fluorophores. Moreover, two-photon cross sections obtained in SEHRS from adenine exceed by far the two-photon fluorescence cross sections encountered for common biomolecules.

Due to the electromagnetic origin of the enhancement, it should be possible to achieve SERS cross sections for other DNA bases in the same order of magnitude as obtained for adenine when they are attached to colloidal silver or gold clusters.

As shown in Fig. 4, the nucleotide bases show well-distinguished surface-enhanced Raman spectra. This suggests DNA sequencing based on SERS [34]. After cleaving single native nucleotides from the DNA strand into a medium containing colloidal silver or gold clusters, direct detection and identification of single native nucleotides should be possible, due to unique SERS spectra of its bases. It is interesting to estimate the detection rate of single nucleotides in such an experiment. Single molecule

**Fig. 4** Schematic of DNA sequencing based on the intrinsic Raman spectra of the four bases G, A, T, and C (spectra are shown in the boxes). After cleaving single native nucleotides from the DNA strand into a moving stream of silver or gold nano clusters, single nucleotides will meet SERS-active silver or gold nanoclusters in the sequence of cleaving. Nucleotides are detected and identified when nucleotide loaded nanoclusters move through a laser spot and give rise to characteristic specific SERS signatures. Reprinted with permission from Ref. [11]

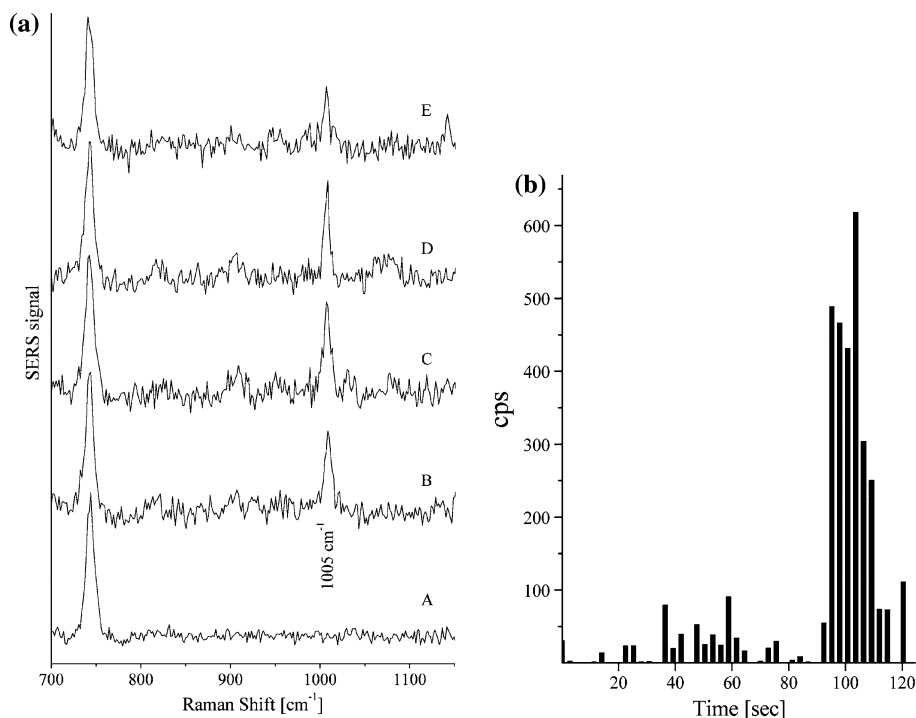


adenine spectra can be measured at good signal-to-noise ratios of 10 in 1-s collection time at  $3 \times 10^5$  W/cm<sup>2</sup> excitation. Assuming a SERS cross section on the order of  $10^{-17}$  to  $10^{-16}$  cm<sup>2</sup> and a vibrational lifetime on the order of 10 ps, saturation of SERS will be achieved at  $10^8$  to  $10^9$  W/cm<sup>2</sup> excitation intensity. Extrapolation to saturation conditions shows that single molecule SERS spectra over the complete fingerprint region (ca 700–1,700 cm<sup>-1</sup>) should be measurable in milliseconds or at kHz rates. This opens spectacular potential applications for rapid DNA sequencing at the single molecule level [34].

In general, identification of a molecule is based on a SERS spectrum, comprised of different vibrational modes, but also measuring only one typical SERS line and using this Raman line as a spectroscopic signature for the specific molecule is a useful tool for detecting and tracking a known molecule without the use of fluorescence labels.

Figure 5 demonstrates this by monitoring the small protein enkephalin on a fractal silver surface [35]. Enkephalin is a mixture of two pentapeptides, [Leu]enkephalin and [Met]enkephalin. As Fig. 5 shows, enkephalin can be monitored at the single molecule level based on the strongly enhanced ring breathing mode of phenylalanine around 1,000 cm<sup>-1</sup>, which is a building block of both the pentapeptides. The SERS signal of the strongly enhanced mode of phenylalanine can be used as intrinsic marker for detecting a single enkephalin molecule without the use of a specific label.

**Fig. 5** **a** SERS spectra with one enkephalin molecule in the focal spot measured in a spectral window, which displays the 1,000 cm<sup>-1</sup> SERS line of phenylalanine. The line at about 750 cm<sup>-1</sup>, which can be ascribed to a citrate impurity on the surface demonstrates the uniform signal level for “many molecules”. **b** Raman signal measured at 1,000 cm<sup>-1</sup> from the same spot in a time sequence (1-s collection time each). The characteristic changes in scattering signal between noise level (see for example spectrum A) and a relatively uniform signal (see spectra B–E) can be explained by diffusion of single enkephalin molecules. Reprinted with permission from Ref. [35]



### 1.3 SERS nanosensors for chemical- and pH-probing in live cells

Probing cellular structures and cellular processes on the molecular level and at subendosomal resolution is one of the major methodological challenges in cell biology [36, 37]. Gold nanoparticles have been tools of the trade in cell biology studies because of its favorable physical and chemical properties and biocompatibility. An exciting new aspect in its applications exploits gold nanoparticles as multifunctional SERS nanosensors. These mobile sensors can probe cellular chemistry at subendosomal resolution by delivering the enhanced Raman spectra of cellular molecules in their nanoenvironment [38, 39]. Figure 6 illustrates the principle of a SERS sensor.

The ultrasensitive detection and structural characterization of molecules in a live cell provides key information for monitoring cellular processes, such as enzymatic activity or release of neurotransmitters [40].

As a further development of SERS nanosensors, gold nanoparticles with reporter molecules attached, which exhibit a known and calibrated pH dependent SERS signature, can also act as intracellular pH meter. SERS spectra measured from 4-mercapto benzoic acid (pMBA) show such pH dependence due to dissociation of the carboxyl group at higher pH values [41]. The line at 1,423 cm<sup>-1</sup> (see spectra in Fig. 7) belongs to the COO<sup>-</sup> stretching mode and can be used as an indicator for the dissociation of the carboxyl group at higher pH values. Signal ratios of the

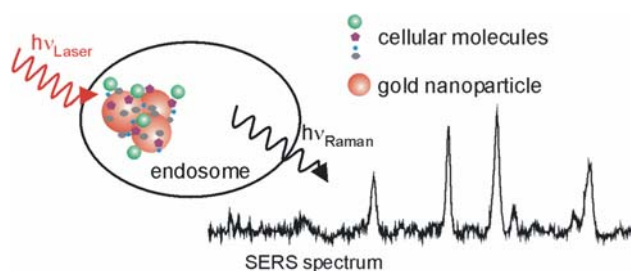


**Fig. 6** High resolution sensors for sensitive cellular probing (schematic). Gold nanoaggregates deliver SERS spectra of cellular molecules in its nano environment. In most cases, the nanoparticles are applied via the cell culture medium. Reprinted with permission from Ref. [39]

$1,423\text{ cm}^{-1}$  to an aromatic ring vibration at  $1,076\text{ cm}^{-1}$  can be used to generate a calibration curve of the pH sensor [42–44]. Figure 7 demonstrates pH measurements in a live cell using such a SERS nanosensor.

As Fig. 7 shows, the SERS signal of pMBA can be analyzed in order to allow one to differentiate between various pH values within the endosomal compartment of a eukaryotic cell.

The concept of a SERS-based pH sensor can be extended to two-photon excitation using surface-enhanced hyper Raman scattering (SEHRS) of pMBA. The pH sensor based on two-photon excitation benefits not only from all advantages related to excitation in the near infrared, but also additionally, compared to SERS, SEHRS spectra of pMBA exhibit a spectral signature that allows an extension of the accessible pH range. Compared to other optical pH sensors based on one- or two-photon excited fluorescence,

which in most cases require the application of multiple probes to cover wider pH ranges, the same SERS/SEHRS sensor can operate between pH values of 8 and 2 enabling the probing of a variety of cellular compartments including those of extreme pH, e.g., very acidic lysosomes. Based on Raman scattering, SERS and SEHRS pH sensors deliver strong signals also under electronically non-resonant excitation. This avoids photodecomposition of the sensor and allows free selection of the excitation wavelengths optimized for the biological object under study.

As a particular advantage for applications in biological environment, SERS/SEHRS pH nanosensors infer information using the relative signals of spectrally narrow “pairs” of Raman lines in the same spectrum (see for example the  $1,423\text{ cm}^{-1}$  and  $1,076\text{ cm}^{-1}$  line in Fig. 7). This allows quantitative measurement without any correction regarding cellular background absorption and emission signals.

#### 1.4 Surface-enhanced Raman optical activity for probing the chiral character of biomolecules on nanostructures and on surfaces

Chirality has become the theme of increasing interest during the recent years. Demand for chiral recognition and separation has increased due to the importance of chirality in many fields, particularly also in biomedical research and pharmaceuticals. Numerous biotic events, ranging from pharmacological aspects of chiral drugs [45] to the origins of life on Mars [46] are being investigated by studies of enantiomeric composition.

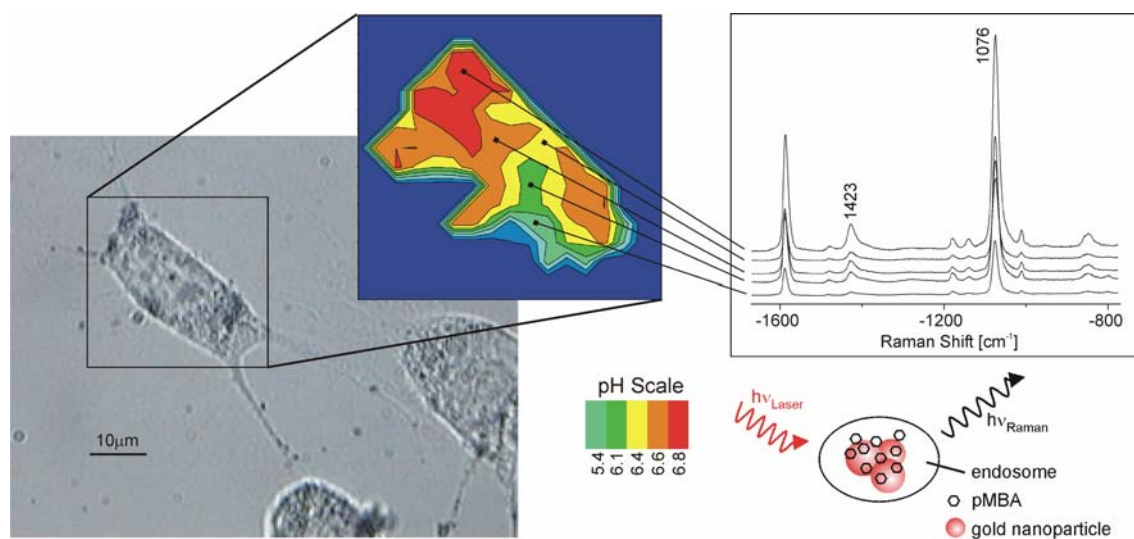


**Fig. 7** Probing and imaging pH values in single live cells using a SERS nanosensor, which exploits the pH sensitive SERS spectrum of the reporter 4-mercapto benzoic acid (pMBA) on gold nanoaggregates. The *left hand side* shows the photomicrograph of an NIH/3T3 cell incubated with the pMBA gold nanosensors. The *color image*

displays a pH map of the cell shown as false color plot of the pH sensitive ratios of the SERS lines. The *right hand side* shows the SERS spectra collected in the cellular compartments exhibiting different pH. Spectra were collected in 1 s each using 3 mW 830 nm cw excitation. Reprinted with permission from Ref. [44]

Different spectroscopic methods are applied to achieve the analysis of chiral enantiomeric compounds [47]. The effect of ROA is particularly sensitive to chirality and provides important information on the chiral character of a molecule based on differences in Raman spectra generated by left- and right-circularly polarized light [48–50].

Here, we discuss ROA measurements performed in local optical fields of silver nanoparticles. Figure 8 shows a surface-enhanced ROA spectrum measured from adenine adsorbed on silver nanoparticles.

To explain the measured ROA spectra, we must assume that adenine adsorbed on the silver nanoparticles forms a chiral structure. The free planar adenine molecule has a single mirror plane and has been regarded as a “prochiral” molecule. The spectral signature of measured SEROA spectra are in good agreement with theoretical calculations performed for adenine adsorbed on small silver clusters recently reported [51]. The computation indicate the existence of two strong SEROA signatures at 730 and 1,330  $\text{cm}^{-1}$  showing opposite sign as it had been found experimentally [52].

Interestingly, the ROA signature of adenine attached to silver surfaces is similar to features in the ROA spectrum of poly(rA) at positions of adenine vibrations. This suggests formation of ordered structures similar to those of adenine in poly(rA). For example, adenine rows were observed on a Cu(110) surface [53].

The SEROA spectrum shown in Fig. 8 was generated from one spectrum for each polarization collected over 10 s using 50 mW, 514.5 nm excitation. The concentration of adenine in silver colloidal solution was 10  $\mu\text{g}/\text{mL}$

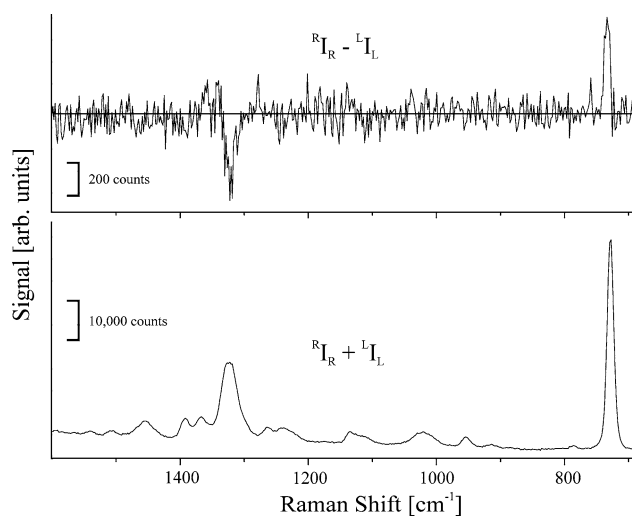


**Fig. 8** a SEROA (top trace) and SERS (bottom trace) spectra of  $8 \times 10^{-5}$  M adenine in silver colloidal solution calculated from spectra measured with right and left circularly polarized excitation and scattered light  $^R I_R$  and  $^L I_L$ . Reprinted with permission from Ref. [52]

( $8 \times 10^{-5}$  M). For comparison, ROA spectra of molecules of biological interest are typically measured using 700–1,000 mW excitation and hours collection time at typical concentrations of the target molecule of tens of  $\text{mg}/\text{mL}$  [54]. These numbers indicate the enormous improvement in experimental conditions of SEROA compared to ROA.

Measuring ROA signals under such improved experimental conditions is possible because of two effects. First, Raman signals are surface enhanced in the local optical fields of the silver nanoparticles, resulting in improved conditions for the collection of very good signal-to-noise Raman spectra. Second, as it was inferred above, the values of CID were found to be of the order of  $10^{-2}$ , i.e., one magnitude higher than the best values reported for classical ROA. Increased CIDs for molecules adsorbed on metal surfaces have been discussed theoretically in terms of large field gradients, in which the Raman scattering takes place [55–57]. Our experimental results confirm this prediction.

As our experimental results and recent computation indicate that there might exist a so-called “surface-induced chirality” for adsorbed molecules. This suggests that caution needs to be practiced in interpreting SEROA spectra regarding conclusions on the chirality of the non-adsorbed molecule. On the other hand, ROA measurements in combination with SERS have the capability to provide unique information on the internal structure, organization, and molecular orientation of molecules on surfaces.

## 2 Conclusion

This article discusses some examples of how surface-enhanced Raman scattering, i.e., Raman scattering in local optical fields of gold and silver nanostructures can advance Raman spectroscopic methods for biophysical and biomedical applications.

Most exciting for biophysical studies might be the trace analytical capabilities of SERS, which enable to establish the molecular identity at the single molecule level. This is of great interest since biologically relevant molecules are often available for characterization in extremely small amounts only. For example, a spectroscopic way for characterizing very small amounts of DNA would open exciting opportunities for reducing or even avoiding PCR amplification.

Identification and structural characterization of an unknown molecule is based on its unique vibrational fingerprint, which usually contains several spectral features. But for detecting and tracking a known molecule one single strong Raman line of the target molecule can be used. For example, the reported result (see Fig. 5) suggests the use of the phenylalanine 1,000  $\text{cm}^{-1}$  SERS line as spectroscopic signature for monitoring single proteins containing this amino acid as a building block.

SERS opens up exciting capabilities for developing biocompatible SERS nanosensors for transducing chemical information from different cellular compartment within individual live cells. Additionally, SERS nanosensors can deliver information on the acidity in different endosomes. Determining and monitoring pH in cells and cellular compartments is of particular importance for a better understanding of a broad range of physiological and metabolic processes. In particular, a combination of molecular structural information together with monitoring the pH value in a live cell as it can be delivered by SERS sensors provides a new means to improve our understanding of cellular processes on the molecular level.

Surface-enhanced Raman measurements can also advance information on the chiral character of molecules. Detection limits in ROA measurements can be improved and data collection times and excitation powers can be considerably reduced by exploiting the effect of surface enhancement. In particular, ROA measurements in combination with SERS have the capability to provide a sensitive tool for probing organization and self-assembling of biologically active molecules on surfaces. This is of particular interest in the growing field of nanobiotechnology. Here, the development of biocompatible materials and biosensors requires a better understanding of the behavior and organization of organic molecules at surfaces. Moreover, chiral organization of molecules on surfaces is becoming a topic of basic scientific interest [58, 59].

**Acknowledgments** We would like to thank the reviewers and the editor for useful comments and suggestions for improving our manuscript.

## References

- Gitai Z (2009) New fluorescence microscopy methods for microbiology: sharper, faster, and quantitative. *Curr Opin Microbiol* 12:341–346
- Xing Y, Xia ZY, Rao JH (2009) Semiconductor quantum dots for biosensing and in vivo imaging. *IEEE Trans Nanobiosci* 8:4–12
- Laserna JJ (1996) *Modern techniques in Raman spectroscopy*. Wiley, Chichester, New York, Brisbane, Toronto, Singapore
- Puppels GJ, Mul FFMD, Otto C, Greve J, RobertNicoud M, Arndt-Jovin DJ, Jovin T (1990) Studying single living cells and chromosomes by confocal Raman microspectroscopy. *Nature* 347:301–303
- Hanlon EB, Manoharan R, Koo TW, Shafer KE, Motz JT, Fitzmaurice M, Kramer JR, Itzkan I, Dasari RR, Feld MS (2000) Prospects for in vivo Raman spectroscopy. *Phys Med Biol* 45:R1–R59
- Kneipp J, Bakker Schut TC, Kliffen M, Menke-Pluijmers M, Puppels GJ (2003) Characterization of breast duct epithelia: a Raman spectroscopic study. *Vib Spectrosc* 32:67–74
- Kneipp J, Miller LM, Joncic M, Kittel M, Lasch P, Beekes M, Naumann D (2003) In situ identification of protein structural changes in prion-infected tissue. *Biochim Biophys Acta* 1639:152–158
- Scepanovic OR, Fitzmaurice M, Gardecki JA, Angheloiu GO, Awasthi S, Motz JT, Kramer JR, Dasari RR, Feld MS (2006) Detection of morphological markers of vulnerable atherosclerotic plaque using multimodal spectroscopy. *J Biomed Opt* 11(2):021003
- Kneipp K (2007) Surface-enhanced Raman scattering. *Phys Today* 60:40–46
- Kneipp K, Kneipp H, Itzkan I, Dasari RR, Feld MS (2002) Surface-enhanced Raman scattering and biophysics. *J Phys Condens Matter* 14:R597–R624
- Kneipp K, Kneipp H (2006) Single molecule Raman scattering. *Appl Spectrosc* 60:322A–334A
- Stuart AD, Yuen JM, Shah NC, Lyandres O, Yonzon CR, Glucksberg MR, Walsh JT, Van Duyne RP (2006) In vivo glucose measurement by surface-enhanced Raman spectroscopy. *Anal Chem* 78:7211–7215
- Qian XM, Nie SM (2008) Single-molecule and single-nanoparticle SERS: from fundamental mechanisms to biomedical applications. *Chem Soc Rev* 37:912–920
- Kneipp J, Kneipp H, Kneipp K (2008) SERS—a single-molecule and nanoscale tool for bioanalytics. *Chem Soc Rev* 37:1052–1060
- Hering K, Cialla D, Ackermann K, Dorfer T, Moller R, Schneidewind H, Mattheis R, Fritzsche W, Rosch P, Popp J (2008) SERS: a versatile tool in chemical and biochemical diagnostics. *Anal Bioanal Chem* 390:113–124
- Qian XM, Peng XH, Ansari DO, Yin-Goen Q, Chen GZ, Shin DM, Yang L, Young AN, Wang MD, Nie SM (2008) In vivo tumor targeting and spectroscopic detection with surface-enhanced Raman nanoparticle tags. *Nat Biotechnol* 26:83–90
- Anker JN, Hall WP, Lyandres O, Shah NC, Zhao J, Van Duyne RP (2008) Biosensing with plasmonic nanosensors. *Nat Mater* 7:442–453
- Hudson SD, Chumanov G (2009) Bioanalytical applications of SERS (surface-enhanced Raman spectroscopy). *Anal Bioanal Chem* 394:679–686
- Scaffidi JP, Gregas MK, Seewaldt V, Vo-Dinh T (2009) SERS-based plasmonic nanobiosensing in single living cells. *Anal Bioanal Chem* 393:1135–1141
- Barron LD, Zhu FJ, Hecht L, Tranter GE, Isaacs NW (2007) Raman optical activity: an incisive probe of molecular chirality and biomolecular structure. *J Mol Struct* 834:7–16
- Nafie LA (1996) Vibrational optical activity in focus. *Appl Spectrosc* 50:A12–A12
- Haesler J, Schindelholz I, Riguet E, Bochet CG, Hug W (2007) Absolute configuration of chirally deuterated neopentane. *Nature* 446:526–529
- Otto A (1984) Surface-enhanced Raman scattering: ‘classical’ and ‘chemical’ origins. In: Cardona M, Guntherodt G (eds) *Light scattering in solids IV. Electronic scattering, spin effects, SERS and morphic effects*, vol 1984. Springer, Berlin, pp 289–418
- Moskovits M (1985) Surface-enhanced spectroscopy. *Rev Mod Phys* 57:783–826
- Campion A, Kambhampati P (1998) Surface-enhanced Raman scattering. *Chem Soc Rev* 27:241–250
- Stockman MI, Shalaev VM, Moskovits M, Botet R, George TF (1992) Enhanced Raman scattering by fractal clusters: scale-invariant theory. *Phys Rev B* 46:2821–2830
- Li KR, Stockman MI, Bergman DJ (2003) Self-similar chain of metal nanospheres as an efficient nanolens. *Phys Rev Lett* 91:227402
- Schatz GC, Young MA, Van Duyne RP (2006) Electromagnetic mechanism of SERS. In: *Surface-enhanced Raman scattering: physics and applications*, vol 103. Springer, Berlin, pp 19–45
- Kneipp J, Kneipp H, Kneipp K (2006) Two-photon vibrational spectroscopy for biosciences based on surface-enhanced hyper-Raman scattering. *Proc Natl Acad Sci USA* 103:17149–17153

30. So PTC, Dong CY, Masters BR, Berland KM (2000) Two-photon excitation fluorescence microscopy. *Ann Rev Biomed Eng* 2:399–429
31. Kobat D, Durst ME, Nishimura N, Wong AW, Schaffer CB, Xu C (2009) Deep tissue multiphoton microscopy using longer wavelength excitation. *Opt Express* 17:13354–13364
32. Schade R, Weiss T, Liefelth K (2009) Two-photon techniques in tissue engineering. *Int J Artif Organs* 32:394
33. Stepanenko I, Kompanetz V, Makhneva Z, Chekalin S, Moskalenko A, Razjivin A (2009) Two-photon excitation spectroscopy of carotenoid-containing and carotenoid-depleted LH2 complexes from purple bacteria. *J Phys Chem B* 113:11720–11723
34. Kneipp K, Kneipp H, Kartha VB, Manoharan R, Deinum G, Itzkan I, Dasari RR, Feld MS (1998) Detection and identification of a single DNA base molecule using surface-enhanced Raman scattering (SERS). *Phys Rev E* 57:R6281–R6284
35. Kneipp K, Kneipp H, Abdali S, Berg RW, Bohr H (2004) Single molecule Raman detection of enkephalin on silver colloidal particles. *Spectrosc Int J* 18:433–440
36. Kneipp J (2006) Nanosensors based on SERS for applications in living cells. In: *Surface-enhanced Raman scattering: physics and applications*, vol 103. Springer, Berlin, pp 335–349
37. Chourpa I, Lei FH, Dubois P, Manfait M, Sockalingum GD (2008) Intracellular applications of analytical SERS spectroscopy and multispectral imaging. *Chem Soc Rev* 37:993–1000
38. Kneipp J, Kneipp H, Rice WL, Kneipp K (2005) Optical probes for biological applications based on surface-enhanced Raman scattering from indocyanine green on gold nanoparticles. *Anal Chem* 77:2381–2385
39. Kneipp J, Kneipp H, McLaughlin M, Brown D, Kneipp K (2006) In vivo molecular probing of cellular compartments with gold nanoparticles and nanoaggregates. *Nano Lett* 6:2225–2231
40. Dijkstra RJ, Scheenen W, Dam N, Roubos EW, ter Meulen JJ (2007) Monitoring neurotransmitter release using surface-enhanced Raman spectroscopy. *J Neurosci Methods* 159:43–50
41. Michota A, Bukowska J (2003) Surface-enhanced Raman scattering (SERS) of 4-mercaptobenzoic acid on silver and gold substrates. *J Raman Spectrosc* 34:21–25
42. Bishnoi SW, Rozell CJ, Levin CS, Gheith MK, Johnson BR, Johnson DH, Halas NJ (2006) All-optical nanoscale pH meter. *Nano Lett* 6:1687–1692
43. Talley CE, Jusinski L, Hollars CW, Lane SM, Huser T (2004) Intracellular pH sensors based on surface-enhanced Raman scattering. *Anal Chem* 76:7064–7068
44. Kneipp J, Kneipp H, Wittig B, Kneipp K (2007) One- and two-photon excited optical pH probing for cells using surface-enhanced Raman and hyper-Raman nanosensors. *Nano Lett* 7:2819–2823
45. Muller N, Payan E, Lopicque F, Bannwarth B, Netter P (1990) Pharmacological aspects of chiral nonsteroidal antiinflammatory drugs. *Fundam Clin Pharmacol* 4:617–634
46. Skelley AM, Scherer JR, Aubrey AD, Grover WH, Ivester RHC, Ehrenfreund P, Grunthaler FJ, Bada JL, Mathies RA (2005) Development and evaluation of a microdevice for amino acid biomarker detection and analysis on Mars. *Proc Natl Acad Sci USA* 102:1041–1046
47. Kumar AP, Jin D, Lee YI (2009) Recent development on spectroscopic methods for chiral analysis of enantiomeric compounds. *Appl Spectrosc Rev* 44:267–316
48. Barron LD, Buckingham AD (1971) Raman optical activity. *Mol Phys* 20:1111
49. Deplazes E, van Bronswijk W, Zhu F, Barron LD, Ma S, Nafie LA, Jalkanen KJ (2008) A combined theoretical and experimental study of the structure and vibrational absorption, vibrational circular dichroism, Raman and Raman optical activity spectra of the *L*-histidine zwitterion. *Theor Chem Acc* 119:155–176
50. Jalkanen KJ, Degtyarenko IM, Nieminen XC, Nafie LA, Zhu F, Barron LD (2008) Role of hydration in determining the structure and vibrational spectra of *L*-alanine and *N*-acetyl *L*-alanine *N'*-methylamide in aqueous solution: a combined theoretical and experimental study. *Theor Chem Acc* 119:191–210
51. Jensen L (2009) Surface-enhanced vibrational Raman optical activity: a time-dependent density functional theory approach. *J Phys Chem A* 113:4437–4444
52. Kneipp H, Kneipp J, Kneipp K (2006) Surface enhanced Raman optical activity (SEROA) on adenine in silver colloidal solution. *Anal Chem* 78:1363
53. Chen Q, Frankel DJ, Richardson NV (2002) Self-assembly of adenine on Cu(110) surfaces. *Langmuir* 2002:3219–3225
54. Barron LD, Hecht L, McColl IH, Blanch EW (2004) Raman optical activity comes of age. *Mol Phys* 102:731–744
55. Sass JK, Neff H, Moskovits M, Holloway S (1981) Electric field gradient effects on the spectroscopy of adsorbed molecules. *J Phys Chem* 85:621–623
56. Efrima S (1983) The effect of large electric-field gradients on the Raman optical-activity of molecules adsorbed on metal-surfaces. *Chem Phys Lett* 102:79–82
57. Efrima S (1985) Raman optical-activity of molecules adsorbed on metal-surfaces—theory. *J Chem Phys* 83:1356–1362
58. Humblot V, Barlow SM, Raval R (2004) Two-dimensional organisational chirality through supramolecular assembly of molecules at metal surfaces. *Prog Surf Sci* 76:1–19
59. Humblot V, Raval R (2005) Chiral metal surfaces from the adsorption of chiral and achiral molecules. *Appl Surf Sci* 241:150–156